

# Performance Evaluation of Improved Energy Detection under Signal and Noise Uncertainties in Cognitive Radio Networks

Bansi Gajera\*, Dhaval K. Patel\*, Brijesh Soni\*, Miguel López-Benítez<sup>†‡</sup>

\*School of Engineering and Applied Science, Ahmedabad University, Ahmedabad, India

<sup>†</sup>Department of Electrical Engineering and Electronics, University of Liverpool, United Kingdom

<sup>‡</sup>ARIES Research Centre, Antonio de Nebrija University, Spain

Email: bansi.g.btech15@ahduni.edu.in, dhaval.patel@ahduni.edu.in,

brijesh.soni@ahduni.edu.in, m.lopez-benitez@liverpool.ac.uk

**Abstract**—Energy detection has proved to be a promising technique for spectrum sensing owing to its simplicity and low implementation and computational costs. However, the signals present in the sensed band are ambiguous and are not fully known beforehand which is referred to as the signal uncertainty. Signal and noise uncertainties are prone to degrade the detection performance. This paper presents an analysis of the impact of signal and noise uncertainties under an Improved Energy Detection (IED) algorithm for spectrum sensing. Step by step derivation and analysis of signal detection with signal and noise uncertainties under the considered IED algorithm are carried out in detail. The obtained analytical results are compared with experimental results obtained with a spectrum measurement platform, which not only demonstrate the validity of the mathematical analysis presented in this work but also show that IED outperforms the classical energy detection algorithm even in presence of both signal and noise uncertainties, an important fact of practical relevance that had not been demonstrated to the date in the existing literature.

**Index Terms**—Cognitive radio, Improved energy detection, Low SNR regime, Noise uncertainty, Signal uncertainty

## I. INTRODUCTION

Cognitive radio (CR) has been foreseen as an effective and reliable solution for the efficient utilization of the radio spectrum. The spectrum unavailability issue arising due to static and exclusive frequency allocation can be alleviated using CR. CR is a radio network technology that has knowledge of its operational and geographical environment and adapts to it intelligently to provide a highly reliable communication [1], [2]. With the help of CR, unlicensed users can access the spectrum temporarily unexploited by the licensed user in a non-interfering manner.

The spectrum sensing act of reliably and autonomously identifying the unused frequency bands is foreseen as one of the main functionalities of CRs [3]. Several spectrum sensing algorithms have been proposed to reliably and autonomously identify the unused frequency [4]–[8]. A CR user in most cases is unaware of the primary signals present in its sensed frequency band. The energy detection (ED) technique of spectrum sensing doesn't require any prior information of the primary signals and has been one of the most preferred approach

due to its simple implementation and low computation costs. The classical energy detection (CED) is the simplest energy-based algorithm for spectrum sensing. Enhanced energy-based algorithms of modified energy detection (MED) and improved energy detection (IED) [9] outperforms the well-known CED method. The interest of this work is in the IED method, which outperforms the previously proposed algorithms.

Factors like sensing time, accuracy of the decision made regarding channel occupancy, fundamental limits in the sensing algorithm due to uncertainties, shadowing and hidden PU problems characterizes the sensing algorithm. As uncertain factors commonly exist in practical networks, a perfect knowledge of the signals present in the sensed band is not possible. In ED, the receiver has no prior information about the primary signal being detected and its features such as the energy variation pattern. This is commonly referred to as *signal uncertainty* (SU) [10]. Apart from SU, there exists *noise uncertainty* (NU) arising as a result of the inability to quantify the system noise perfectly [10]. The ED performance degrades heavily under NU conditions, in particular in the low SNR regime [11], [12]. A spectrum sensing system with dynamic noise variance was described in terms of a dynamic state space model in [13]. Uncertainties impose fundamental limitations upon the sensing event and could lead to faulty decisions. Hence, uncertainties can't be neglected and ought to be considered whilst analyzing the overall performance of spectrum sensing algorithms.

The potential effects that both SU and NU may have on the practical performance of the CED algorithm were analyzed in [10]. However, while broadly used in the literature, CED provides in general a poor detection performance. Other methods such as IED have been shown to outperform CED significantly at no extra cost. However the impact of SU and NU on IED has not been investigated yet. In this context, this work fills the existing gap by providing a detailed mathematical and experimental performance evaluation of the IED algorithm under both SU and NU, and compares the performance of IED to the CED method under the effect of both degrading effects (as opposed to the study presented in [9] where the IED

TABLE I: Notation used in this work.

Parameter	Definition
$P_d$	Probability of detection
$P_{fa}$	Probability of false alarm
$P_{md}$	Probability of mis-detection
$\gamma$	Signal to noise ratio (SNR)
$\gamma_0$	Average SNR
$N$	Sensing sample size
$L$	Number of last sensing events considered
$M$	Number of sensing events where a primary signal was actually present
$\alpha$	Noise uncertainty parameter
$\beta$	Signal uncertainty parameter

method was proposed, where IED and CED were compared assuming ideal conditions for both signal and noise powers).

The major contributions of this work are as follows:

- Firstly, a comprehensive analysis of the fundamental bounds on the detection performance in low SNR regime in the presence of both SU and NU when using IED is presented. A closed-form expression is obtained analytically to model the average detection probability of IED considering the impact of SU and NU at the CR receiver.
- Secondly, the validity and accuracy of the obtained analytical results are corroborated using empirical measurement data obtained with an experimental hardware setup.
- Thirdly, we investigate the computational complexity of both methods (CED and IED) under both scenarios (with and without uncertainties) and demonstrate that their respective computational complexities are not affected significantly by the presence of uncertainties.

The rest of the paper is organized as follows. First, Section II introduces the concept of spectrum sensing in the context of ED and provides an overview of the theoretical performance of IED under NU conditions. Section III then incorporates the impact of SU into the analysis and derives a closed-form expression for the detection probability based on a generic mathematical model for the received SNR under variable primary transmission power patterns, which is formulated and approximated by a modified Gaussian distribution. Section IV presents the hardware setup employed in this work to capture the empirical data used to validate the obtained analytical results. Section V presents and provides a detailed discussion of the obtained theoretical and experimental results. Finally, Section VI summarizes the main findings of this work. The notation employed in this work is summarized in Table I.

## II. THEORETICAL PERFORMANCE OF IED UNDER NOISE UNCERTAINTY

The decision to be made regarding the occupancy of the channel can be represented with a binary hypothesis model, namely  $H_0$  (null hypothesis) and  $H_1$  (alternative hypothesis):

$$\begin{aligned} H_0 : y(n) &= w(n) & n &= 1, 2, 3, \dots, N \\ H_1 : y(n) &= x(n) + w(n) & n &= 1, 2, 3, \dots, N \end{aligned} \quad (1)$$

where,  $y(n)$  represents the received signal at  $n$ -th instant,  $w(n)$  is the AWGN noise and  $x(n)$  represents the transmitted signal. Here  $H_0$  states that primary signal are absent in the sensed spectrum band, and hypothesis  $H_1$  indicates the presence of some licensed user signal  $x(n)$ .  $N$  denotes the number of samples collected during the signal observation interval (i.e., the sensing sample size).

NU mostly resulting from varying thermal noise in components caused by temperature variations (non-uniform, time-varying), noise due to transmissions by other users or noise power calibration errors is likely to affect the practical networks. Variations in the noise power adds NU in the CR [14]. The noise power is uncertain and this can be modelled within a range [15] as  $\hat{\sigma}_w^2 \in [\sigma_w^2, \alpha\sigma_w^2]$ , where  $\hat{\sigma}_w^2$  is the estimated noise power,  $\sigma_w^2$  is the nominal noise power and  $\alpha > 1$  is the NU parameter.

The detection probability of IED under AWGN for perfectly known signal and noise powers was presented in [9]. The introduction of NU in the analysis presented in [9] leads to the following new result for the detection probability of IED in the presence of NU as a function of the SNR (derivation details are omitted due to the lack of space):

$$P_d^{IED}(\gamma) = Q(\zeta(\gamma)) + Q(\zeta(\gamma))(1 - Q(\zeta(\gamma)))Q(\xi(\gamma)) \quad (2)$$

where  $Q(\zeta(\gamma))$  represents the probability of detection of the CED algorithm, which under NU is obtained to be given by:

$$Q(\zeta(\gamma)) = Q\left(\frac{\alpha Q^{-1}(P_{fa})\sqrt{2N} - N(\gamma + 1 - \alpha)}{\sqrt{2N}(1 + \gamma)}\right) \quad (3a)$$

while the term  $Q(\xi(\gamma))$  is given by:

$$Q(\xi(\gamma)) = Q\left(\frac{\alpha Q^{-1}(P_{fa})\sqrt{2N} - \frac{MN}{L}\gamma + (\alpha - 1)N}{\sqrt{\frac{2N}{L}\left(1 + \frac{M}{L}\left[(1 + \gamma)^2 - 1\right]\right)}}\right) \quad (3b)$$

where  $Q(\cdot)$  is the Gaussian  $Q$ -function,  $P_{fa}$  represents the target probability of false alarm,  $\gamma$  is the SNR,  $L$  is the number of sensing events over which the IED algorithm is run, and  $M$  is the number of sensing events (out of the considered  $L$  sensing events) where a primary signal was actually present. The Gaussian  $Q$ -function is defined as  $Q(x) = \frac{1}{2}\text{erfc}\left(\frac{x}{\sqrt{2}}\right)$ , where  $\text{erfc}(\cdot)$  is the complementary error function such that  $\text{erfc}(x) = \frac{2}{\sqrt{\pi}} \int_x^\infty e^{-t^2} dt$ .

In low SNR regime ( $\gamma \ll 1$ ), these expressions reduce to:

$$Q(\zeta(\gamma)) \approx Q\left(\alpha Q^{-1}(P_{fa}) - \sqrt{\frac{N}{2}}(\gamma + 1 - \alpha)\right) \quad (3c)$$

$$Q(\xi(\gamma)) \approx Q\left(\alpha Q^{-1}(P_{fa})\sqrt{L} - M\sqrt{\frac{N}{2L}}\gamma + (\alpha - 1)\sqrt{\frac{NL}{2}}\right) \quad (3d)$$

Since  $\alpha \geq 1$  and the  $Q$ -function is a decreasing function of its argument, it can be observed from (3) that  $P_d$  for the IED algorithm degrades under NU and decreases with an increase in the uncertainty parameter  $\alpha$ . With an increase in the sensing

sample size  $N$ , the value of the  $Q$ -function increases and so does the resulting detection probability.

### III. THEORETICAL PERFORMANCE OF IED UNDER BOTH NOISE AND SIGNAL UNCERTAINTIES

This section extends the result introduced in Section II by taking account the impact of the SU on the detection performance of the IED method, thus providing a closed-form expression for its detection probability under both SU and NU.

In real scenarios, the SNR at the CR receiver depends on both the propagation environment and the primary transmission power pattern. The transmission power of the primary user may vary over time, which would lead to a varying SNR at the CR receiver even under an ideal propagation channel. Moreover, the propagation channel introduces attenuation, shadowing and multipath fading, which leads to additional fluctuations in the instantaneous SNR observed at the CR receiver. Since the detection probability depends on the SNR, its instantaneous value will fluctuate as well. The average detection probability  $\bar{P}_d^{IED}$  for an average SNR  $\gamma_0$ , which would be a more meaningful parameter in this case, can be computed as:

$$\bar{P}_d^{IED}(\gamma_0) = \mathbb{E}[P_d^{IED}(\gamma)] = \int_{\gamma} P_d^{IED}(\gamma) f_{\gamma}(\gamma) d\gamma \quad (4)$$

where  $P_d^{IED}(\gamma)$  is the detection probability for an instantaneous SNR  $\gamma$  as given by (2) and  $f_{\gamma}(\gamma)$  is the probability density function (PDF) of the instantaneous SNR. The focus of this work being on the primary transmission power pattern (i.e., SU), it is assumed that  $f_{\gamma}(\gamma)$  is mostly due to the primary transmission power pattern. An exact expression for  $f_{\gamma}(\gamma)$  cannot be determined since this would require a perfect knowledge of the primary transmission power statistics, which is not known to the CR receiver. However, based on the empirical results obtained in [16], it was concluded in [10] that  $f_{\gamma}(\gamma)$  can be accurately modelled in most practical cases with either a Rayleigh or a gamma distribution. For these two distributions, the variance and the average value are related by a constant factor. Concretely, the variance of the instantaneous SNR,  $\sigma_{\gamma}^2$ , can be written in terms of the average SNR,  $\gamma_0$ , as  $\sigma_{\gamma}^2 = \beta\gamma_0^2$  [10], where  $\beta = \sigma_{\gamma}^2/\gamma_0^2 > 0$  can be regarded as the normalized variance of the received SNR, which can be used to quantify the uncertainty of the received primary signal at the CR receiver (i.e., the SU). The value of  $\beta$  is constant for the Rayleigh ( $\beta \approx 0.27$ ) and gamma ( $\beta \approx 0.5$ ) distributions and therefore these models are not suitable for scenarios with variable SU levels. In order to model the effect of SU for any arbitrary  $\beta$ , a truncated modified Gaussian PDF is employed in this work, whose PDF is defined as follows [10]:

$$f_{\gamma}(\gamma) \approx \frac{K}{\sqrt{2\pi}\sigma_{\gamma}} e^{-\frac{1}{2}\left(\frac{\gamma-\gamma_0}{\sigma_{\gamma}}\right)^2}, \quad \gamma > 0 \quad (5)$$

where  $K$  is a normalization factor required by the truncation of the original Gaussian distribution, which is given by:

$$K = \frac{2}{1 + \operatorname{erf}\left(\frac{\gamma_0}{\sqrt{2}\sigma_{\gamma}}\right)} \quad (6)$$

where  $\operatorname{erf}(\cdot)$  is the Gaussian error function. The variance of this modified Gaussian distribution is independent of the average SNR and therefore can be employed to quantify any arbitrary level of SU at the CR receiver through  $\beta = \sigma_{\gamma}^2/\gamma_0^2$ .

The average probability of detection for the IED algorithm under both SU and NU can be obtained by introducing the expression obtained in (2)–(3), which only accounts for the NU, into the integral in (4), which would lead to a result that also includes the impact of SU (i.e., both SU and NU). Given the analytical complexity of the resulting integral, a number of approximations are needed. First, the expression in (2) needs to be used along with the low SNR approximations in (3c) and (3d). In most practical scenarios, CR devices are expected to operate under low SNR conditions, therefore this assumption is reasonable (an indeed, it has been commonly used in the literature). Secondly, the Gaussian  $Q$ -Function can be approximated using a second-order exponential function as follows [17]:

$$Q(x) \approx \begin{cases} e^{-(ax^2+bx+c)}, & x \geq 0 \\ 1 - e^{-(ax^2-bx+c)}, & x < 0 \end{cases} \quad (7)$$

where  $a = 0.3845$ ,  $b = 0.7635$  and  $c = 0.6966$  are fitting coefficients [17]. Introducing (7) into (3c),  $Q(\zeta(\gamma))$  can be further approximated as:

$$Q(\zeta(\gamma)) \approx \begin{cases} e^{-(a[\zeta(\gamma)]^2+b\zeta(\gamma)+c)} \\ = e^{-(\Omega\gamma^2+\Psi\gamma+\Phi)}, & \zeta(\gamma) \geq 0 \\ 1 - e^{-(a[\zeta(\gamma)]^2-b\zeta(\gamma)+c)} \\ = 1 - e^{-(\Omega\gamma^2+\Xi\gamma+\theta)}, & \zeta(\gamma) \leq 0 \end{cases} \quad (8)$$

where:

$$\Omega = \frac{aN}{2}$$

$$\Psi = -a\alpha Q^{-1}(P_{fa})\sqrt{2N} - aN(\alpha - 1) - b\sqrt{\frac{N}{2}}$$

$$\Xi = -a\alpha Q^{-1}(P_{fa})\sqrt{2N} - aN(\alpha - 1) + b\sqrt{\frac{N}{2}}$$

$$\Phi = a \left[ \alpha Q^{-1}(P_{fa}) + (\alpha - 1) \sqrt{\frac{N}{2}} \right]^2 + b \left[ \alpha Q^{-1}(P_{fa}) + (\alpha - 1) \sqrt{\frac{N}{2}} \right] + c$$

$$\theta = a \left[ \alpha Q^{-1}(P_{fa}) + (\alpha - 1) \sqrt{\frac{N}{2}} \right]^2 - b \left[ \alpha Q^{-1}(P_{fa}) + (\alpha - 1) \sqrt{\frac{N}{2}} \right] + c$$

Similarly, introducing (7) into (3d),  $Q(\xi(\gamma))$  can be further approximated as follows:

$$Q(\xi(\gamma)) \approx \begin{cases} e^{-(a[\xi(\gamma)]^2+b\xi(\gamma)+c)} \\ = e^{-(\Omega_1\gamma^2+\Psi_1\gamma+\Phi_1)}, & \xi(\gamma) \geq 0 \\ 1 - e^{-(a[\xi(\gamma)]^2-b\xi(\gamma)+c)} \\ = 1 - e^{-(\Omega_1\gamma^2+\Xi_1\gamma+\theta_1)}, & \xi(\gamma) \leq 0 \end{cases} \quad (9)$$

where:

$$\begin{aligned}\Omega_1 &= \frac{aN M^2}{2L} \\ \Psi_1 &= -a\alpha Q^{-1}(P_{fa})M\sqrt{2N} - aMN(\alpha - 1) - bM\sqrt{\frac{N}{2L}} \\ \Xi_1 &= -a\alpha Q^{-1}(P_{fa})M\sqrt{2N} - aMN(\alpha - 1) + bM\sqrt{\frac{N}{2L}} \\ \Phi_1 &= a \left[ \alpha\sqrt{L}Q^{-1}(P_{fa}) + (\alpha - 1)\sqrt{\frac{NL}{2}} \right]^2 \\ &\quad + b \left[ \alpha\sqrt{L}Q^{-1}(P_{fa}) + (\alpha - 1)\sqrt{\frac{NL}{2}} \right] + c \\ \theta_1 &= a \left[ \alpha\sqrt{L}Q^{-1}(P_{fa}) + (\alpha - 1)\sqrt{\frac{NL}{2}} \right]^2 \\ &\quad - b \left[ \alpha\sqrt{L}Q^{-1}(P_{fa}) + (\alpha - 1)\sqrt{\frac{NL}{2}} \right] + c\end{aligned}$$

With the approximations described above, the average probability of detection for the IED algorithm under both SU and NU can be obtained. Concretely, an approximated version of the expression in (2) is obtained by using the approximated form of  $Q(\zeta(\gamma))$  in (8) and the approximated form of  $Q(\xi(\gamma))$  in (9). This approximated version of (2) can then be introduced into (4), while  $f_\gamma(\gamma)$  in (4) is given by the truncated Gaussian model shown in (5). The integral obtained after these substitutions has an algebraic form that is tractable, even though its resolution is quite tedious. After numerous algebraic manipulations, which do not involve major analytical difficulties and are therefore here omitted due to the lack of space, the expression shown in (10) is finally obtained as a result, where  $\text{erf}(\cdot)$  the error function,  $\Upsilon = \alpha\sqrt{2/N}Q^{-1}(P_{fa}) + (\alpha - 1)$ ,  $\Upsilon_1 = (L/M)[\alpha\sqrt{2/N}Q^{-1}(P_{fa}) + \alpha - 1]$ , and:

$$\begin{aligned}\Omega_2 &= \left( \Omega + \Omega_1 + \frac{1}{2\sigma_\gamma^2} \right) & \Omega_3 &= \left( 2\Omega + \Omega_1 + \frac{1}{2\sigma_\gamma^2} \right) \\ \Psi_2 &= \left( \Psi + \Psi_1 - \frac{\gamma_0}{\sigma_\gamma^2} \right) & \Psi_3 &= \left( 2\Psi + \Psi_1 - \frac{\gamma_0}{\sigma_\gamma^2} \right) \\ \Xi_2 &= \left( \Xi + \Xi_1 - \frac{\gamma_0}{\sigma_\gamma^2} \right) & \Xi_3 &= \left( 2\Xi + \Xi_1 - \frac{\gamma_0}{\sigma_\gamma^2} \right) \\ \Phi_2 &= \left( \Phi + \Phi_1 + \frac{\gamma_0^2}{2\sigma_\gamma^2} \right) & \Phi_3 &= \left( 2\Phi + \Phi_1 + \frac{\gamma_0^2}{2\sigma_\gamma^2} \right) \\ \theta_2 &= \left( \theta + \theta_1 + \frac{\gamma_0^2}{2\sigma_\gamma^2} \right) & \theta_3 &= \left( 2\theta + \theta_1 + \frac{\gamma_0^2}{2\sigma_\gamma^2} \right)\end{aligned}$$

Some of the terms in (10) are numerically similar and therefore cancel out each other when the expression is evaluated. This observation leads to the slightly simplified form shown in (11). This approximation is valid over a wide range of SNR values and becomes tighter for high  $N$  and low  $P_{fa}$  values.

#### IV. MEASUREMENT SETUP AND DATA ACQUISITION

The accuracy of the mathematical model developed in this work for the performance of the IED algorithm under both SU

and NU was assessed based on empirical data captured with a spectrum measurement platform (see Fig. 1), which was placed on the roof-top of the School of Engineering and Applied Science (SEAS) of Ahmedabad University. The measurement platform is composed of two measurement setups. Setup I consists of a discone antenna (Diamond D-3000N) and a digital spectrum analyzer (Rigol DSA-875) connected to a control PC. This setup is used to analyze the presence/absence of radio signals by observing the power spectral density on the spectrum analyzer screen when tuned to a particular band. Setup II consists of a discone antenna (Diamond D-3000N) and a USRP N210 connected to a control PC running GNU Radio, which is used to capture the actual spectrum data on those channels where activity is detected with the spectrum analyzer. A Python script executed in GNU Radio is in charge of acquiring raw I/Q signal samples from the USRP. The captured data are stored for subsequent off-line processing in MATLAB. The configuration parameters for the USRP and the spectrum analyzer are shown in Tables II and III, respectively.

#### V. THEORETICAL AND EXPERIMENTAL RESULTS

This section compares the theoretical IED performance with the experimental performance based on empirical data. The analysis was performed for the different radio technologies shown in Table II and similar conclusions were obtained in all cases. However, due to the limited space available, only the results for the captured E-GSM 900 DL signal are shown in this section. Results were obtained for sensing sample sizes  $N = \{10, 100, 1000\}$ . NU was reproduced by shifting the energy detection threshold with respect to its nominal value. The amount of SU is calculated for each measured signal based on its SNR ( $\beta = \sigma_\gamma^2/\gamma_0^2$ ). Measurements were carefully performed to ensure that the impact of fading is minimized (e.g., selecting nearby transmitters with direct line of sight and high SNR conditions) so that the observed signal variability is mostly due to the transmission power pattern of the measured transmitter.

Figs. 2 and 3 illustrate the impact of different parameters on the performance of the IED algorithm by evaluating the Receiver Operating Characteristic (ROC), i.e., the probability of detection as a function of the probability of false alarm, based on the theoretical results obtained in Section III. As it can be appreciated from Fig. 2, where the impact of the SU ( $\beta$ ) and the sample size ( $N$ ) are illustrated, the presence of SU degrades the performance of IED (in particular, the performance is more severely degraded for higher values of the signal variability/uncertainty  $\beta$ ), however this can be overcome by increasing the sample size  $N$ . Fig. 3 shows the impact of  $M$  (number of sensing events over which the IED algorithm is executed where a primary signal is present), indicating that, as expected, a higher value of  $M$  leads to an increased detection performance. This is because the averaging process performed by the IED method can detect a primary signal more reliably when it is present in a higher number of sensing events (again, the detection performance improves with the sample size).

$$\begin{aligned}
\bar{P}_d^{IED}(\gamma_0) \approx & \frac{K}{2} \left\{ \operatorname{erf} \left( \frac{\Upsilon_1 - \gamma_0}{\sqrt{2}\sigma_\gamma} \right) - \operatorname{erf} \left( \frac{\Upsilon - \gamma_0}{\sqrt{2}\sigma_\gamma} \right) + \operatorname{erfc} \left( \frac{\Upsilon_1 - \gamma_0}{\sqrt{2}\sigma_\gamma} \right) \right. \\
& + \sqrt{\frac{1}{2\sigma_\gamma^2\Omega_3}} \exp \left( \frac{\Xi_3^2}{4\Omega_3} - \theta_3 \right) \operatorname{erfc} \left( \frac{2\Omega_3\Upsilon_1 + \Xi_3}{2\sqrt{\Omega_3}} \right) \\
& + \sqrt{\frac{1}{2\sigma_\gamma^2\Omega_2}} \exp \left( \frac{\Xi_2^2}{4\Omega_2} - \theta_2 \right) \operatorname{erfc} \left( \frac{2\Omega_2\Upsilon_1 + \Xi_2}{2\sqrt{\Omega_2}} \right) \\
& - \sqrt{\frac{1}{2\sigma_\gamma^2\Omega_3}} \exp \left( \frac{\Psi_3^2}{4\Omega_3} - \Phi_3 \right) \left[ \operatorname{erf} \left( \frac{2\Omega_3\Upsilon + \Psi_3}{2\sqrt{\Omega_3}} \right) - \operatorname{erf} \left( \frac{\Psi_3}{2\sqrt{\Omega_3}} \right) \right] \\
& \left. + \sqrt{\frac{1}{2\sigma_\gamma^2\Omega_3}} \exp \left( \frac{\Xi_3^2}{4\Omega_3} - \theta_3 \right) \left[ \operatorname{erf} \left( \frac{2\Omega_3\Upsilon_1 + \Xi_3}{2\sqrt{\Omega_3}} \right) - \operatorname{erf} \left( \frac{2\Omega_3\Upsilon + \Xi_3}{2\sqrt{\Omega_3}} \right) \right] \right\} \quad (10)
\end{aligned}$$

$$\begin{aligned}
\bar{P}_d^{IED}(\gamma_0) \approx & \left( \frac{1}{1 + \operatorname{erf} \left( \frac{\gamma_0}{\sqrt{2}\sigma_\gamma} \right)} \right) \left\{ \operatorname{erfc} \left( \frac{\Upsilon_1 - \gamma_0}{\sqrt{2}\sigma_\gamma} \right) \right. \\
& + \sqrt{\frac{1}{2\sigma_\gamma^2\Omega_2}} \exp \left( \frac{\Xi_2^2}{4\Omega_2} - \theta_2 \right) \operatorname{erfc} \left( \frac{2\Omega_2\Upsilon_1 + \Xi_2}{2\sqrt{\Omega_2}} \right) \\
& - \sqrt{\frac{1}{2\sigma_\gamma^2\Omega_3}} \exp \left( \frac{\Psi_3^2}{4\Omega_3} - \Phi_3 \right) \left[ \operatorname{erf} \left( \frac{2\Omega_3\Upsilon + \Psi_3}{2\sqrt{\Omega_3}} \right) - \operatorname{erf} \left( \frac{\Psi_3}{2\sqrt{\Omega_3}} \right) \right] \\
& \left. - \sqrt{\frac{1}{2\sigma_\gamma^2\Omega_3}} \exp \left( \frac{\Xi_3^2}{4\Omega_3} - \theta_3 \right) \operatorname{erf} \left( \frac{2\Omega_3\Upsilon_1 + \Xi_3}{2\sqrt{\Omega_3}} \right) \right\} \quad (11)
\end{aligned}$$

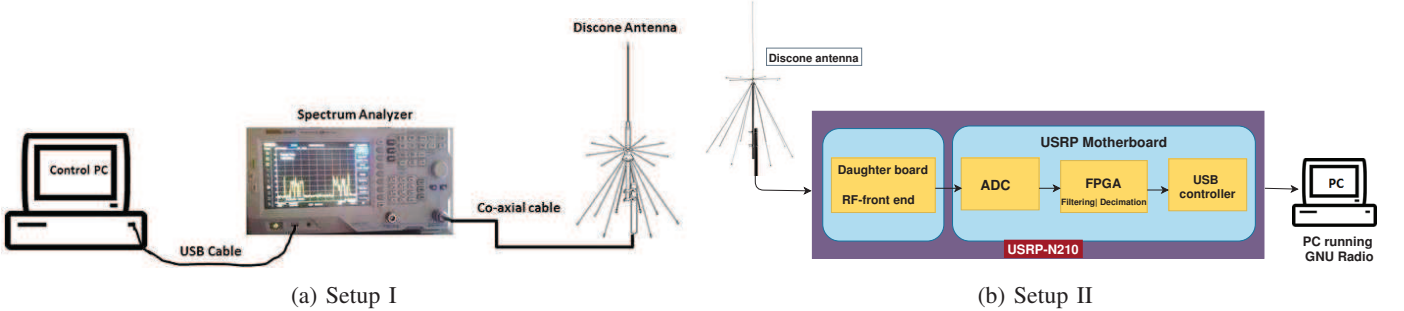


Fig. 1: Spectrum measurement platform used in this work for spectrum data acquisition.

Fig. 4 shows the theoretical and empirical detection probability of both CED and IED as a function of the SNR in the absence of NU, while Fig. 5 shows the counterpart for the case of 1-dB NU. The IED algorithm is executed over blocks of  $L = 3$  sensing events and the theoretical results are plotted for the whole range of  $M = \{1, 2, 3\}$ . Notice that the value of  $M$  in the case of empirical measurements is unknown since the number of sensing events where the primary signal was actually present cannot be determined reliably, therefore  $M$  can only be considered in the case of theoretical results. Nevertheless, it can be observed from Fig. 4 that the empirical IED performance for the scenario without noise uncertainty overlaps perfectly with the theoretical IED performance for  $M = 2$ . This indicates that, in average, the measured primary

signal was present in two out every three sensing events ( $M = 2, L = 3$ ). Moreover, note that this is observed for all the considered values of the samples size  $N$ , which corroborates the validity of the obtained analytical results in Section III. In the case with noise uncertainty (Fig. 5), a slight deviation is observed between the theoretical and experimental IED performances for  $M = 2$ , which can be explained by the difficulty to have a perfect measure of the actual NU as a result of the variability of the noise power at the hardware receiver during the interval over which measurements were carried out. The obtained results show that IED outperforms CED even in the presence of both SU and NU, however the detection performance is lower bounded in both cases by the same SNR wall, which is inherent to the ED principle itself.

TABLE II: USRP configuration and channels measured in this work.

Radio Technology	Channel Number	$f_{start}$ (MHz)	$f_{center}$ (MHz)	$f_{stop}$ (MHz)	Signal bandwidth (MHz)	Gain (dB)	Decimation Rate	Sampled Bandwidth (MHz)
FM broadcasting	–	96.500	96.700	96.900	0.2	45	64	1
UHF television (Band IV)	U-33	566	570	574	8	45	8	8
E-GSM 900 DL	77	950.2	950.4	950.6	0.2	45	64	1
DCS 1800 DL	690	1839.6	1840.8	1841	0.2	45	64	1

TABLE III: Spectrum analyzer configuration.

Parameter	Value
Frequency range	75-2000 MHz
Frequency span	45-600 MHz
Frequency bin	Depends on band selected
Resolution bandwidth (RBW)	10 kHz
Video bandwidth (VBW)	10 kHz
Measurement period	5-15 mins
Sweep time	1 second
Scale	10 dB/division
Input attenuation	0 dB
Detection type	RMS detector

Finally, Fig. 6 shows the experimental computational cost of CED and IED for different sample sizes in terms of the average time required to execute each algorithm on a general purpose processor (Intel i5 Quad Core at 2.66 GHz), averaged over 8000 Monte-Carlo iterations. As it can be appreciated, the computational cost of IED is slightly higher than CED, in particular at lower sample sizes, as a result of the additional calculations required to average the energy values observed over several sensing events. In practice, a relatively large number of signal samples are required to provide a reliable sensing decision, meaning that in most practical scenarios the IED/CED algorithms will be operating in the region of larger sample sizes shown on the right-hand side of Fig. 6, where the computational costs of CED and IED are equivalent. This same behaviour was also observed in [9] in the absence of SU and NU. Interestingly, the results in Fig. 6 show that the computational cost of the IED algorithm is not significantly affected by the presence of SU and NU and, as a result, the performance improvements of IED over CED that were observed [9] at no extra computational cost, are also observed here in the presence of SU and NU, again at no extra cost.

## VI. CONCLUSION

Several energy-based spectrum sensing algorithms have been proposed in the literature with the aim to improve the performance of the well-known CED method. This work focuses on the IED method proposed in [9], which has been shown to outperform CED at no extra computational cost. The performance of the IED method was analyzed in [9] under ideal conditions where the signal and noise powers were assumed to be perfectly known by the CR receiver. On the other hand, this work has provided a more realistic analysis where the impacts of SU and NU on the IED performance have been analyzed mathematically. The obtained analytical results have been compared with experimental data obtained with a

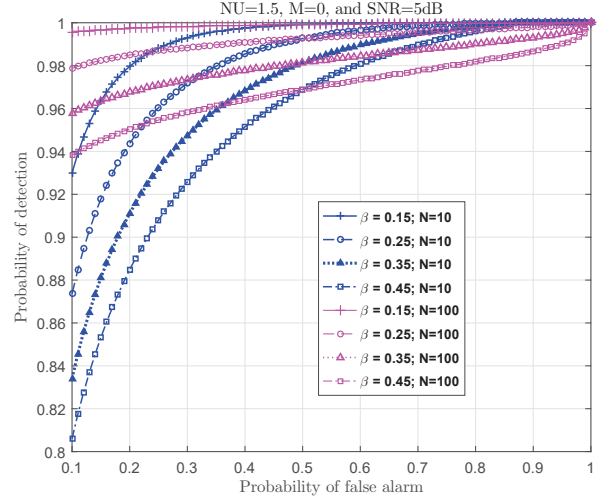


Fig. 2: Theoretical IED performance: impact of  $\beta$  and  $N$ .

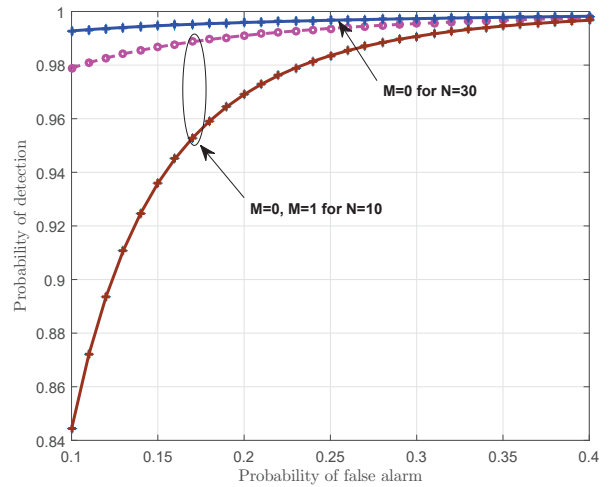


Fig. 3: Theoretical IED performance: impact of  $M$ .

spectrum measurement platform. The obtained results have not only demonstrated the validity of the mathematical analysis presented in this work but also showed that IED outperforms the CED algorithm, not only under ideal conditions but also in presence of both signal and noise uncertainties.

## ACKNOWLEDGEMENT

This work was supported by the DST-UKIERI Programme under Grant DST/INT/UK/P-150/2016. The authors would

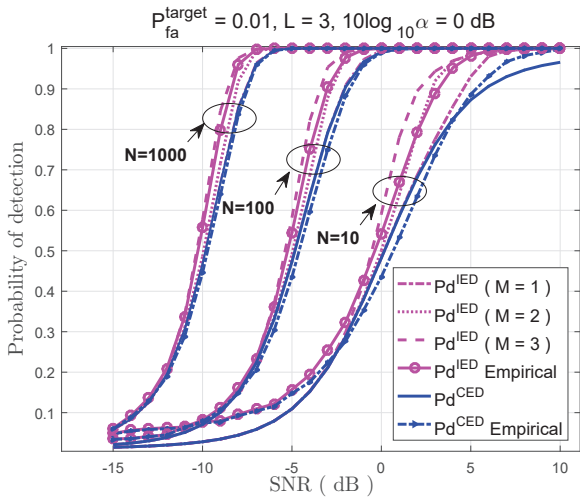


Fig. 4: Theoretical and empirical performance of IED ( $M = \{1, 2, 3\}$ ,  $L = 3$ ) and CED without NU.

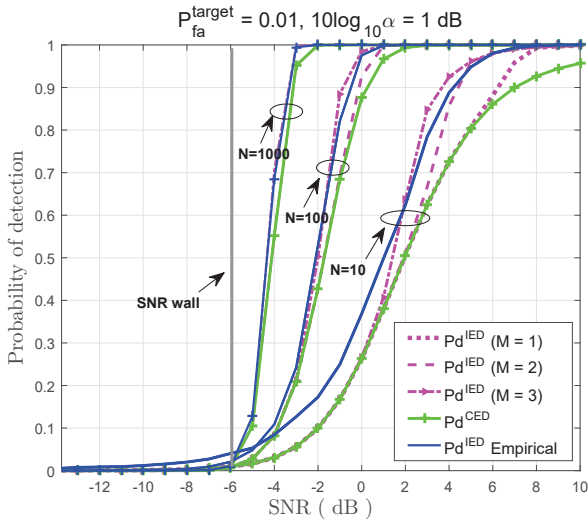


Fig. 5: Theoretical and empirical performance of IED ( $M = \{1, 2, 3\}$ ,  $L = 3$ ) and CED under 1-dB NU.

like to thank Ahmedabad University, India and University of Liverpool, UK for the provided infrastructural support.

#### REFERENCES

- [1] V. T. Nguyen, F. Villain, and Y. Le Guillou, *Cognitive radio RF: Overview and challenges*, VLSI Design. Hindawi, 2012, vol. 2012.
- [2] S. Haykin, "Cognitive radio: brain-empowered wireless communications," *IEEE J. Sel. Areas Commun.*, vol. 23, no. 2, pp. 201–220, Feb 2005.
- [3] T. Yucek and H. Arslan, "A survey of spectrum sensing algorithms for cognitive radio applications," *Proc. IEEE*, vol. 97, no. 5, pp. 805–823, 2009.
- [4] M. Hamid, N. Bjorsell, and S. B. Slimane, "Energy and eigenvalue based combined fully blind self adapted spectrum sensing algorithm," *IEEE Trans. Veh. Technol.*, vol. 65, no. 2, pp. 630–642, 2016.
- [5] F. F. Digham, M.-S. Alouini, and M. K. Simon, "On the energy detection of unknown signals over fading channels," *IEEE Trans. Commun.*, no. 1, pp. 21–24, 2007.

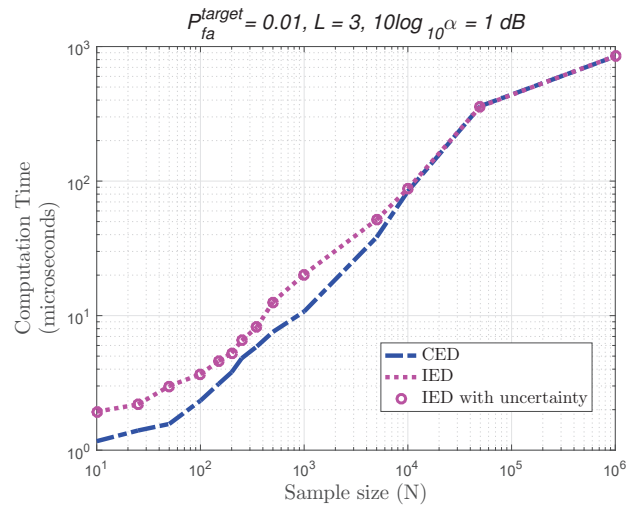


Fig. 6: Computational cost of IED and CED vs. sample size.

- [6] M. R. Manesh, S. Apu, N. Kaabouch, and W.-c. Hu, "Performance evaluation of spectrum sensing techniques for cognitive radio systems," *IEEE Annual Conference on Ubiquitous Computing, Electronics & Mobile Communication*, pp. 1–6, 2016.
- [7] Ying-Chang Liang, Yonghong Zeng, E. Peh, and Anh Tuan Hoang, "Sensing-throughput tradeoff for cognitive radio networks," *IEEE Trans. Wirel. Commun.*, vol. 7, no. 4, pp. 1326–1337, 2008.
- [8] L. Safatly, B. Aziz, A. Nafkha, Y. Louet, Y. Nasser, A. El-Hajj, and K. Y. Kabalan, "Blind spectrum sensing using symmetry property of cyclic autocorrelation function: From theory to practice," *Eurasip Journal on Wireless Communications and Networking*, vol. 2014, 2014.
- [9] M. López-Benítez and F. Casadevall, "Improved energy detection spectrum sensing for cognitive radio," *IET Commun.*, vol. 6, no. 8, p. 785, 2012.
- [10] —, "Signal Uncertainty in Spectrum Sensing for Cognitive Radio," *IEEE Trans. Commun.*, vol. 61, no. 4, pp. 1231–1241, 2013.
- [11] W. Jouini, "Energy detection limits under log-normal approximated noise uncertainty," *IEEE Signal Process. Lett.*, vol. 18, no. 7, pp. 423–426, 2011.
- [12] S. Bahamou and A. Nafkha, "Noise uncertainty analysis of energy detector: Bounded and unbounded approximation relationship," in *21st European Signal Processing Conference (EUSIPCO)*, 2013, pp. 1–4.
- [13] M. Sun, C. Zhao, S. Yan, and B. Li, "A novel spectrum sensing for cognitive radio networks with noise uncertainty," *IEEE Trans. Veh. Technol.*, vol. 66, no. 5, pp. 4424–4429, 2017.
- [14] V. Arthi, R. Ramya, and P. Chakkravarthy, "An optimized energy detection scheme for spectrum sensing in cognitive radio," *Int'l. J. Eng. Res. & Dev.*, vol. 11, no. 04, pp. 2278–67, 2015.
- [15] A. Sahai, N. Hoven, and R. Tandra, "Some fundamental limits on cognitive radio," *Allerton Conference on Control, Communications, and Computation*, pp. 1662–1671, 2004.
- [16] M. López-Benítez, F. Casadevall, and C. Martella, "Performance of spectrum sensing for cognitive radio based on field measurements of various radio technologies," *2010 European Wireless Conference*, pp. 969–977, 2010.
- [17] M. López-Benítez and F. Casadevall, "Versatile, accurate, and analytically tractable approximation for the Gaussian Q-function," *IEEE Transactions on Communications*, vol. 59, no. 4, pp. 917–922, 2011.